

論文 / 著書情報
Article / Book Information

論題	
Title	Laser Wavelength Effect on Size and Morphology of Silicon Nanoparticles Prepared by Laser Ablation in Liquid
著者	P. CHEWCHINDA, 柘植 丈治, 舟窪 浩, 小田原 修, 和田 裕之
Authors	Pattarin Chewchinda, Takeharu Tsuge, Hiroshi Funakubo, Osamu Odawara, Hiroyuki Wada
出典	, 52, , 025001
Citation	Japanese Journal of Applied Physics, 52, , 025001
発行日 / Pub. date	2013, 1
DOI	http://dx.doi.org/10.7567/JJAP.52.025001
URL	https://www.jsap.or.jp/
権利情報 / Copyright	本著作物の著作権は（公社）応用物理学会に帰属します。 (c) 2013 The Japan Society of Applied Physics
Note	このファイルは著者（最終）版です。 This file is author (final) version.

Erratum: “Laser Wavelength Effect on Size and Morphology of Silicon Nanoparticles Prepared by Laser Ablation in Liquid” [Jpn. J. Appl. Phys. 52 (2013) 025001]

Pattarin CHEWCHINDA*, Takeharu TSUGE, Hiroshi FUNAKUBO, Osamu ODAWARA, and Hiroyuki WADA

Department of Innovative and Engineered Materials, Interdisciplinary Graduate School of Science and Engineering, Tokyo Institute of Technology, Yokohama 226-8503, Japan

The equation (6) should be changed from

$$r^* = \frac{2\gamma\Omega}{kT} \ln\left(\frac{C_0}{C}\right)$$

to

$$r^* = \frac{2\gamma\Omega}{kT \ln\left(\frac{C}{C_0}\right)}$$

Laser Wavelength Effect on Size and Morphology of Silicon

Nanoparticles Prepared by Laser Ablation in Liquid

Pattarin CHEWCHINDA*, Takeharu TSUGE, Hiroshi FUNAKUBO,

Osamu ODAWARA, Hiroyuki WADA

Department of Innovative and Engineered Materials, Interdisciplinary

Graduate School of Science and Engineering, Tokyo Institute of

Technology, Yokohama, 226-8503, Japan

The effect of laser wavelength on size and morphology of silicon nanoparticles are studied. To prepare nanoparticles, laser ablation in liquid technique is employed. Absorption spectra demonstrate that with laser wavelength of 532nm, solution with higher concentration can be prepared in comparison with one obtained from laser wavelength of 1064nm. TEM images reveal nanoparticles with spherical shape from samples produced by both laser wavelengths. However, smaller particles size are obtained from sample prepared by laser wavelength of 532nm. Raman spectra and photoluminescence (PL) spectra further support the existence of smaller crystal size in this sample.

*E-mail address: chewchinda.p.aa@m.titech.ac.jp

1. Introduction

Due to its abundance, cheapness, and non-toxicity, silicon nanoparticles are considered as promising material in diverse field of applications.¹⁻⁵⁾ It is reported that silicon quantum dot offers higher multiple exciton generation (MEG) quantum yield at lower photon energy than that of bulk silicon. Besides, MEG occurs at very high rates with higher efficiencies compared to that of impact ionization in bulk semiconductor.⁶⁻⁷⁾ These observations confirm that MEG in silicon quantum dot has the potential to improve conversion efficiency of photovoltaic cell, which is further approved by Kawashima *et al.*²⁾ They found that current density is higher in solar cell with silicon nanoparticles than the cell without them. Another interesting work by Uchida *et al.* reveals that an integration of silicon nanoparticles with ruthenium dye results in an improvement of power conversion efficiency by 3.0% compared with solar cell without those nanoparticles.⁸⁾ They believe that silicon nanoparticles increase effective surface area for Ru-dye attachment and also enhance light absorption in UV region, which finally affect the device performance.

Apart from photovoltaic application, silicon nanoparticles are also an

outstanding material for biological field owing to their non-toxicity and suitable surface for chemical functionalization.⁹⁾ PEG phospholipids micelle-encapsulated silicon quantum dots are found to be relatively stable in various biologically relevant conditions. Moreover, the uptake of these probes shows no observable toxicity.¹⁰⁾ Warner *et al.* reported a simple room-temperature synthesis of water-soluble silicon quantum dots. These nanoparticles are incorporated into HeLa cells to demonstrate its potential in bioimaging application and the result emphasizes the possibility of using these dots in biological fluorescence imaging.¹¹⁾ Besides bioimaging application, silicon nanoparticles are also functionalized in drug delivery system and reveal several remarkable features including high payload, biodegradability, and multiple loading without the need of additional chemical reagents.⁴⁾ Based on these reports, it is obviously demonstrated that highly luminescent and stable silicon quantum dots are excellent candidates for fluorescent biological probes in either long-term or real-time cellular labeling.

In order to modify silicon nanoparticles to meet the requirement of each potential application, the development of their preparation process is a

major concern. Up until now, synthesis of silicon nanoparticles can be realized by several techniques including electrochemical etching;^{4,12-13)} by microemulsion route;¹⁾ by aerosol synthesis;¹⁴⁾ by plasma enhanced chemical vapour deposition;¹⁵⁾ by pulse laser deposition;¹⁶⁻¹⁸⁾ or by laser pyrolysis of silane;^{10,19-22)}. However, these methods either require complicated experimental setup or result in nanoparticles with impurity involved.

To overcome these limitations, laser ablation in liquid has been introduced. With this technique, nanoparticles can be prepared within a single-step process, which is very simple.²³⁻²⁷⁾ Besides, nanoparticles are synthesized in clean environment resulting in outstanding purity of products.^{24,26-30)} In addition, the entire products can be collected within the solution, which simplifies handling.^{25,27)} According to these reasons, laser ablation in liquid is one of the promising technique in the preparation of nanoparticles, especially silicon.

There exists several publications regarding silicon nanoparticles prepared by laser ablation in liquid. Nonetheless, difference in experimental conditions including laser fluence, irradiation time, liquid media, or even solvent layer thickness leads to variation in size and morphology of the

obtained nanoparticles, which affect their properties.^{3,5,23,28,30-38)} In this work, silicon nanoparticles are prepared by employing laser ablation in liquid and the effects of laser wavelength on size and morphology of prepared nanoparticles are studied.

2. Experiment

P-type <100> silicon wafer (resistivity of 11.5-15.5 $\Omega\cdot\text{cm}$ and thickness of 600 μm) is used as a target material, which is cleaned by ultrasonic treatment in ethanol for 20 minutes. This target is then immersed in 2mL of 99.5% ethanol and irradiated for 30 minutes by Q-switch Nd:YAG laser with the first and the second harmonic generation, which corresponds to wavelength of 1064nm and 532nm respectively. Pulse width of both lasers is approximately 10ns with repetition rate of 10Hz. Energy density of both laser can be controlled by the suitable ND filter and is adjusted to be 1.2J/cm² for both cases. Schematic diagram of experimental setup is shown in Fig. 1.

After irradiation, the obtained colloidal solution is dropped onto Cu grid and dried in order to prepare for TEM observation by FE-TEM 2010F microscope. This solution is then transferred into quartz cuvette and

absorption spectra is measured by SIMADZU: MultiSpec1500 spectrometer. Photoluminescence (PL) property is also observed by Hitachi High-Technologies F-7000 fluorescence spectrophotometer with excitation wavelengths of 350nm. Finally, colloidal solution is dropped onto Al pan and dried in order to analyze the composition of nanoparticles by Raman spectroscopy with 514.5nm line of Ar⁺ laser at room temperature.

3. Results

From absorption spectra, as shown in Fig. 2, it is obviously seen that higher absorbance is obtained from the sample prepared by laser wavelength of 532nm compared to one prepared by 1064nm. Following Beer Lambert law

$$A = \epsilon cl, \quad (1)$$

where A is absorbance, ϵ is molar extinction coefficient, c is concentration, and l is path length.³⁹⁾ Since absorbance is directly proportional to concentration, where ϵ and l are fixed as constant, higher concentration is obtained from solution prepared by laser wavelength of 532nm.

Apart from the difference in concentration, absorption spectra also review absorption edge approximately at 400nm and 420nm from the sample

prepared by laser wavelength of 532nm and 1064nm, respectively. These correspond to energy gaps of 3.1eV and 2.95eV. Due to quantum confinement effect, the bandgap increases as the particle size decreases.¹⁸⁾ As a consequence, smaller particle size is expected from the sample prepared by laser wavelength of 532nm.

Nanoparticles prepared by both lasers reveal spherical shape as shown in Fig. 3. In addition, crystallinity is also observed in both cases. Although some agglomeration presents, most of nanoparticles well disperse. From TEM images, the size distribution of nanoparticles prepared by both lasers are constructed by measuring the diameter of 100 nanoparticles. The results, as shown in Fig. 4, indicate that smaller particle size and also narrower distribution are obtained from sample prepared by 532nm, which agrees well with the assumption previously made from absorption spectra result. The average size and standard deviation are summarized in Table I.

From Raman spectra shown in Fig. 5, silicon peak is detected at 518.732cm^{-1} from the sample prepared by laser wavelength of 1064nm. However, the peak reveals at 515.552cm^{-1} from one prepared by laser wavelength of 532nm. After deconvolution of these peaks, their positions

shift to 519.076cm^{-1} and 516.643cm^{-1} respectively. These peak positions are used further to calculate crystal size based on the equation

$$\Delta\omega = -52.3 \left(\frac{0.543}{D} \right)^{1.586}, \quad (2)$$

where $\Delta\omega$ is Raman peak position shift (cm^{-1}) and D is crystal size (nm).^{30,33-}

^{34,37,40)} Note that Raman peak of bulk silicon locates at 520cm^{-1} . Following this estimation, crystal sizes prepared by both lasers are derived in Table II.

Besides crystalline peak, silicon oxide also presents at 497.078cm^{-1} .^{33, 41)}

Fig. 6 shows photoluminescence (PL) spectra of both samples. There exists peak at 413nm for nanoparticles prepared by laser wavelength of 532nm. On the contrary, in the case of those prepared by laser wavelength of 1064nm, peaks are detected at 423nm and 460nm. This red shift indicates that larger particle size is obtained in the latter case.^{19,42-43)}

It is reported that nanoparticles size should be smaller than 2nm in order to achieve blue emission.¹¹⁾ In this work, however, not all particles are within this range. One possible explanation for this is oxide-related defects which might be formed in the surface of silicon nanoparticles, which is supported by raman spectra result. Under this circumstance, there is a possibility that electron-hole pairs recombine at this defect state, which

finally leads to blue emission.

4. Discussion

Absorption spectra suggest that higher concentration is obtained from the sample prepared by laser wavelength of 532nm compared to one prepared by laser wavelength of 1064nm. One possible explanation for this different concentration is the difference in optical absorption heat of silicon target at each wavelength. As stated in the following equation

$$H_A = \alpha_0 \varphi_{ph} h\nu = \alpha_0 \frac{I_{opt}}{h\nu} h\nu = \alpha_0 I_{opt}, \quad (3)$$

where H_A is optical absorption heat, α_0 is absorption coefficient, φ_{ph} is photon flux density, h is Planck's constant, ν is frequency, and I_{opt} is optical wave intensity or power density.⁴⁴⁾ Since power density of both laser is fixed, the optical absorption heat depends only on absorption coefficient of material. In addition, for silicon, absorption coefficient is higher at wavelength of 532nm than at that of 1064nm.⁴⁵⁾ As a consequence, higher optical absorption heat is obtained in the former case. In other words, more energy is available for particles generation.

When laser irradiates on silicon target, its energy will be absorbed on

the surface leading to surface melting, vaporization, and ionization.⁴⁶⁾ Within the pulse duration, high-temperature, high-intensity, and high-pressure plasma plume of silicon atoms ignites over laser spot of the target.^{24,37,47)} Once generated, this plume expands adiabatically at a super sonic velocity due to absorbing later laser pulse, and shock wave is created.^{24,26)} After the pulse terminated, the plume expands resulting in rapid cooling and the formation of silicon nuclei.^{24,37)} These nuclei continue to grow until nearby silicon clusters are completely consumed, and eventually suppress the growth process.^{5,23)}

Based on nucleation and growth theory,

$$\Delta G_v = -\frac{kT}{\Omega} \ln\left(\frac{C}{C_0}\right), \quad (4)$$

where ΔG_v is the change of Gibbs free energy per unit volume of solid phase, k is Boltzmann constant, T is temperature, Ω is atomic volume, C is solute concentration, and C_0 is solubility.⁴⁸⁾ Also,

$$r^* = -\frac{2\gamma}{\Delta G_v}, \quad (5)$$

where r^* is minimum size of stable spherical nucleus and γ is surface energy per unit area.⁴⁸⁾ Substitute eq. (4) into eq. (5) leads to

$$r^* = \frac{2\gamma\Omega}{kT} \ln\left(\frac{C_0}{C}\right). \quad (6)$$

From this expression, it is obviously seen that higher concentration results in smaller critical size of nuclei. Besides, as the concentration increases, more nuclei can be formed.⁴⁸⁾ This means more nuclei can share an additionally supplied of silicon atoms, which finally leads to smaller particle size in the sample prepared by laser wavelength of 532nm.³⁷⁾ In addition, since silicon has higher absorption at wavelength of 532nm, there is a possibility that fragmentation might occur. This could be another reason for smaller particles size obtained at this wavelength.

5. Conclusion

Silicon nanoparticles are successfully prepared by laser ablation in ethanol using Nd:YAG laser with different wavelength of 1064nm and 532nm. Distinctive absorption of silicon target at specific wavelength leads to different concentration, which finally influences on particle size. However, no significant difference in morphology is observed.

Acknowledgement

We would like to appreciate Prof. Kazutaka NAKAMURA for laser

equipment and also Mr. Katsuaki HORI for TEM observation (Center for Advanced Materials Analysis, Tokyo Institute of Technology). In addition, we would like to show our gratitude to Mr. Yoshitaka EHARA and Miss Ayumi WADA for their kindly support and invaluable assistance. This work is carried out in Materials and Structure Laboratory (Tokyo Institute of Technology) as collaborative research and is supported by JSPS KAKENHI Grant Number 23119506.

References

- [1] W. L. Liong, S. Sreekantan, and S. D. Hutagalung: Proc. of SPIE **7743** (2010) 774306–1.
- [2] Y. Kawashima, K. Nakahara, H. Sato, G. Uchida, K. Koga, M. Shiratani, and M. Kondo: Transact. Mater. Res. Soc. Jpn. **35** (2010) 597.
- [3] S. Yang, W. Cai, G. Liu, H. Zeng, and P. Liu: J. Phys. Chem. C **113** (2009) 6480.
- [4] F. De Angelis, A. Pujia, C. Falcone, E. Iaccino, C. Palmieri, C. Liberale, F. Mecarini, P. Candeloro, L. Luberto, A. de Laurentiis, G. Das, G. Scala, and E. Di Fabrizio: Nanoscale **2** (2010) 2230.
- [5] V. Švrček, T. Sasaki, Y. Shimizu, and N. Koshizaki: Journal of Laser Micro/Nanoengineering **2** (2007) 15.
- [6] A. J. Nozik: Chem. Phys. Lett. **457** (2008) 3.
- [7] M. C. Beard, K. P. Knutsen, P. Yu, J. M. Luther, Q. Song, W. K. Metzger, R. J. Ellingson, and A.J. Nozik: Nano Lett. **7** (2007) 2506.
- [8] G. Uchida, Y. Kawashima, K. Yamamoto, M. Sato, K. Nakahara, T. Matsunaga, D. Yamashita, H. Matsuzaki, K. Kamataki, N. Itegaki, K. Koga, M. Kondo, and M. Shiratani: Phys. Status Solidi C **8** (2011) 3021.

[9] Pavesi, L & Turan, R. *Silicon Nanocrystals: Fundamentals, Synthesis and Applications* (Wiley, Weinheim, 2010) p.508.

[10] F. Erogbogbo, K. T. Yong, I. Roy, G. Xu, P. N. Prasad, and M. T. Swihart: ACS Nano **2** (2008) 873.

[11] J. H. Warner, A. Hoshino, K. Yamamoto, and R. D. Tilley: Angewandte Chemie (International ed. in English) **44** (2005) 4550.

[12] V. Švrček, I. Turkevych, K. Hara, and M. Kondo: Nanotechnology **21** (2010) 215203.

[13] M. V. Wolkin, J. Jorne, and P. M. Fauchet: Phys. Rev. Lett. **82** (1999) 197.

[14] J. Heitmann, F. Müller, M. Zacharias, and U. Gösele: Adv. Mater. **17** (2005) 795.

[15] X. L. Wu, G. G. Siu, S. Tong, X. N. Liu, F. Yan, S. S. Jiang, X. K. Zhang, and D. Feng: Appl. Phys. Lett. **69** (1996) 523

[16] X. Y. Chen, Y. F. Lu, Y. H. Wu, B. J. Cho, M. H. Liu, D. Y. Dai, and W. D. Song: J. Appl. Phys. **93** (2003) 6311.

[17] J. H. Kim

, K. A. Jeon, E. S. Shim, S. Y. Lee: Mater. Sci. Eng. B **89** (2002) 70.

- [18] J. H. Kim, K. A. Jeon, J. B. Choi, S. Y. Lee: *Mater. Sci. Eng. B* **101** (2003) 146.
- [19] S. Botti, R. Coppola, F. Gourbilleau, and R. Rizk: *J. Appl. Phys* **88** (2000) 3396.
- [20] G. Ledoux, O. Guillois, D. Porterat, C. Reynaud, F. Huisken, B. Kohn, and V. Paillard: *Phys. Rev. B* **62** (2000) 15942
- [21] C. Meier, A. Gondorf, S. Lüttjohann, and A. Lorke: *J. Appl. Phys.* **101** (2007) 103112.
- [22] C. Meier, S. Lüttjohann, V. G. Kravets, H. Nienhaus, A. Lorke, and H. Wiggers: *Physica E* **32** (2006) 155.
- [23] V. Švrček, T. Sasaki, Y. Shimizu, and N. Koshizaki: *Appl. Phys. Lett.* **89** (2006) 213113
- [24] P. Liu, H. Cui, C. X. Wang, and G. W. Yang: *Phys. Chem. Chem. Phys.* **12** (2010) 3942
- [25] P. A. Perminov, I. O. Dzhun, A. A. Ezhov, S. V. Zaboltnov, L. A. Golovan, G. D. Ivlev, E. I. Gatskevich, V. L. Malevich, and P. K. Kashkarov: *Laser Phys.* **21** (2011) 801
- [26] Y. Jiang, P. Liu, Y. Liang, H. B. Li, and G. W. Yang: *Appl. Phys. A* **105**

(2011) 903.

[27] V. Švrček, M. Kondo, K. Kalia, and D. Mariotti: Chem. Phys. Lett. **478**

(2009) 224.

[28] D. Rioux, M. Laferrière, A. Douplik, D. Shah, L. Lilge, A. V. Kabashin,
and M. M. Meunier, J. Biomed. Opt. **14** (2011) 021010.

[29] C. L. Sajti, R. Sattari, B. N. Chichkov, and S. Barcikowski: J. Phys.
Chem. C **114** (2010) 2421.

[30] R. Intartaglia, K. Bagga, F. Brandi, G. Das, A. Genovese, E. Di Fabrizio,
and A. Diaspro: J. Phys. Chem. C **115** (2011) 5102.

[31] V. Švrček, D. Mariotti, and M. Kondo: Opt. Express **17** (2009) 520.

[32] S. Zhu, Y. F. Lu, and M. H. Hong: Appl. Phys. Lett. **79** (2001) 1396.

[33] K. Abderrafi, R. G. Calzada, M. B. Gongalsky, I. Suárez, R. Abarques,
V. S. Chirvony, V. Y. Timoshenko, R. Ibáñez, and J. P. Martínez-Pastor: J.
Phys. Chem. C **115** (2011) 5147.

[34] S. Yang, W. Cai, H. Zeng, and Z. Li: J. Appl. Phys. **104** (2008) 023516.

[35] V. Švrček and M. Kondo: Appl. Surf. Sci. **255** (2009) 9643.

[36] P. G. Kuzmin, G. A. Shafeev, V. V. Bukin, S. V. Garnov, C. farcau, R.
Carles, B. Warot-Fontrose, V. Guieu, and G. Viau: J. Phys. Chem. C **114**

(2010) 15266.

[37] S. Yang, W. Cai, H. Zhang, X. Xu, and H. Zeng: *J. Phys. Chem. C* **113**

(2009) 19091.

[38] I. Umezu, H. Minami, H. Senoo, and A. Sugimura: *J. Phys. Conf. Ser.*

59 (2007) 392.

[39] Nair, A. J. *Principles of Biotechnology*. (Laxmi, New Delhi, 2010) p.

264.

[40] S. Li, S. J. Silvers, and M. S. El-shall: *J. Phys. Chem. B* **101** (1997)

1794.

[41] C. J. Brinker, D. R. Tallant, E. P. Roth, and C. S. Ashley: *J. Non-Cryst.*

Solids **82** (1986) 117.

[42] H. Takagi, H. Ogawa, Y. Yamazaki, A. Ishizaki, and T. Nakagiri: *Appl.*

Phys. Lett. **56** (1990) 2379.

[43] R. K. Soni, L. F. Fonseca, O. Resto, M. Buzaianu, and S. Z. Weisz: *J.*

Lumin. **83-84** (1999) 187.

[44] J. Piprek: *Semiconductor Optoelectronic devices: Introduction to*

Physics and Simulation. (Elsevier Science, California, 2003) p. 146.

[45] M. A. Green and M. J. Keevers: *Prog. Photovoltaics* **3** (1995) 189.

[46] M. S. Tillack, D. W. Blair, and S. S. Harilal: *Nanotechnology* **15** (2004)

390.

[47] F. Mafuné, J. Kohno, Y. Takeda, and T. Kondow: *J. Phys. Chem. B* **104**

(2000) 9111.

[48] G. Z. Cao: *Nanostructures&Nanomaterials: Synthesis, Properties&Applications*. (Imperial College Press, London, 2004) Chap. 3.

Figure Captions

Fig. 1 Experimental setup

Fig. 2 Absorption spectra of sample prepared by laser wavelength of 1064nm (solid line) and 532nm (dash line)

Fig. 3 TEM images of nanoparticles prepared by laser wavelength of (a) 1064nm (b) 532nm. Crystallinity of individual nanoparticles (c)

Fig. 4 Size distribution of nanoparticles prepared by laser wavelength of (a) 1064nm and (b) 532nm

Fig. 5 Raman spectra of sample prepared by laser wavelength of 1064nm (solid line) and 532nm (dash line)

Fig. 6 PL spectra of sample prepared by laser wavelength of 1064nm (solid line) and 532nm (dash line)

Tables

Table I Average size and standard deviation of nanoparticles prepared by
both lasers

Laser	Average Size (nm)	Standard Deviation (nm)
1064nm	6.98	4.36
532nm	3.01	1.21

Table II Crystal size of nanoparticles prepared by both lasers

Laser	Crystal Size (nm)
1064nm	6.92
532nm	3.07

Figures

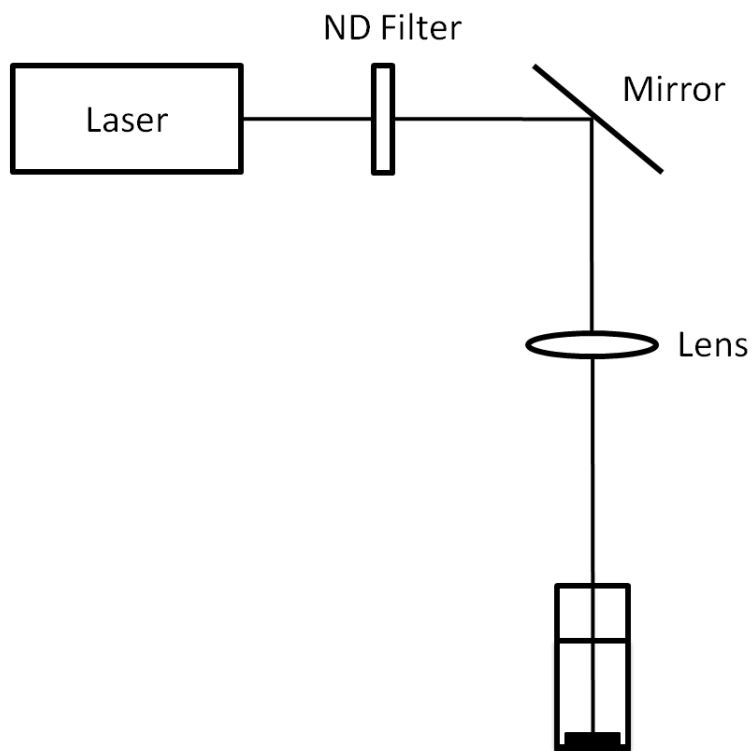


Fig. 1 Experimental setup

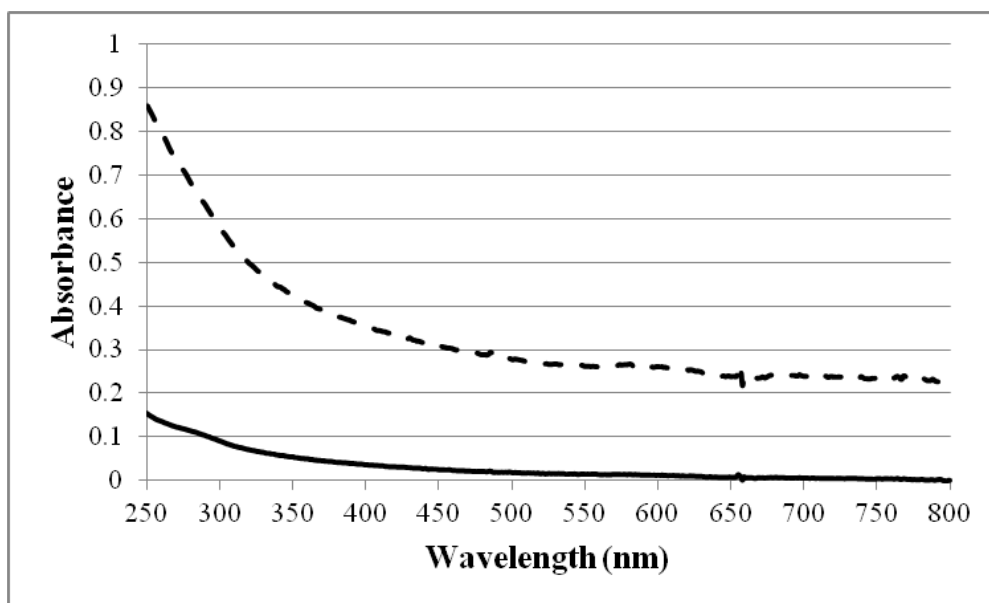


Fig. 2 Absorption spectra of sample prepare by laser wavelength of

1064nm (solid line) and 532nm (dash line)

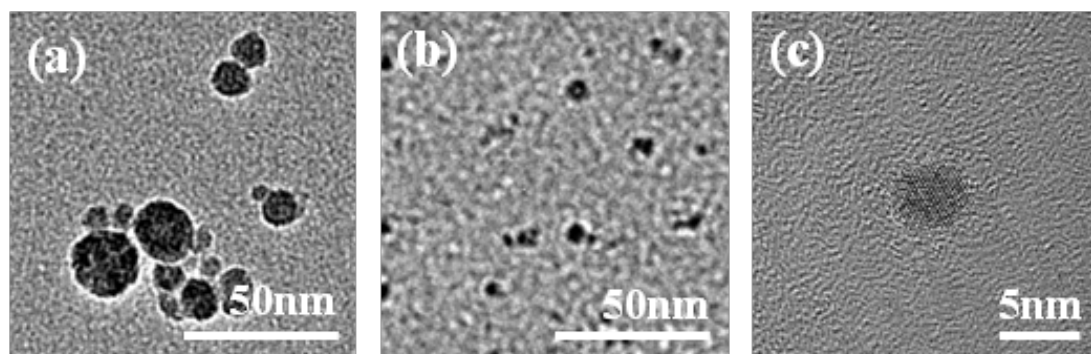


Fig. 3 TEM images of nanoparticles prepared by laser wavelength of (a) 1064nm (b) 532nm. Crystallinity of individual nanoparticles (c)

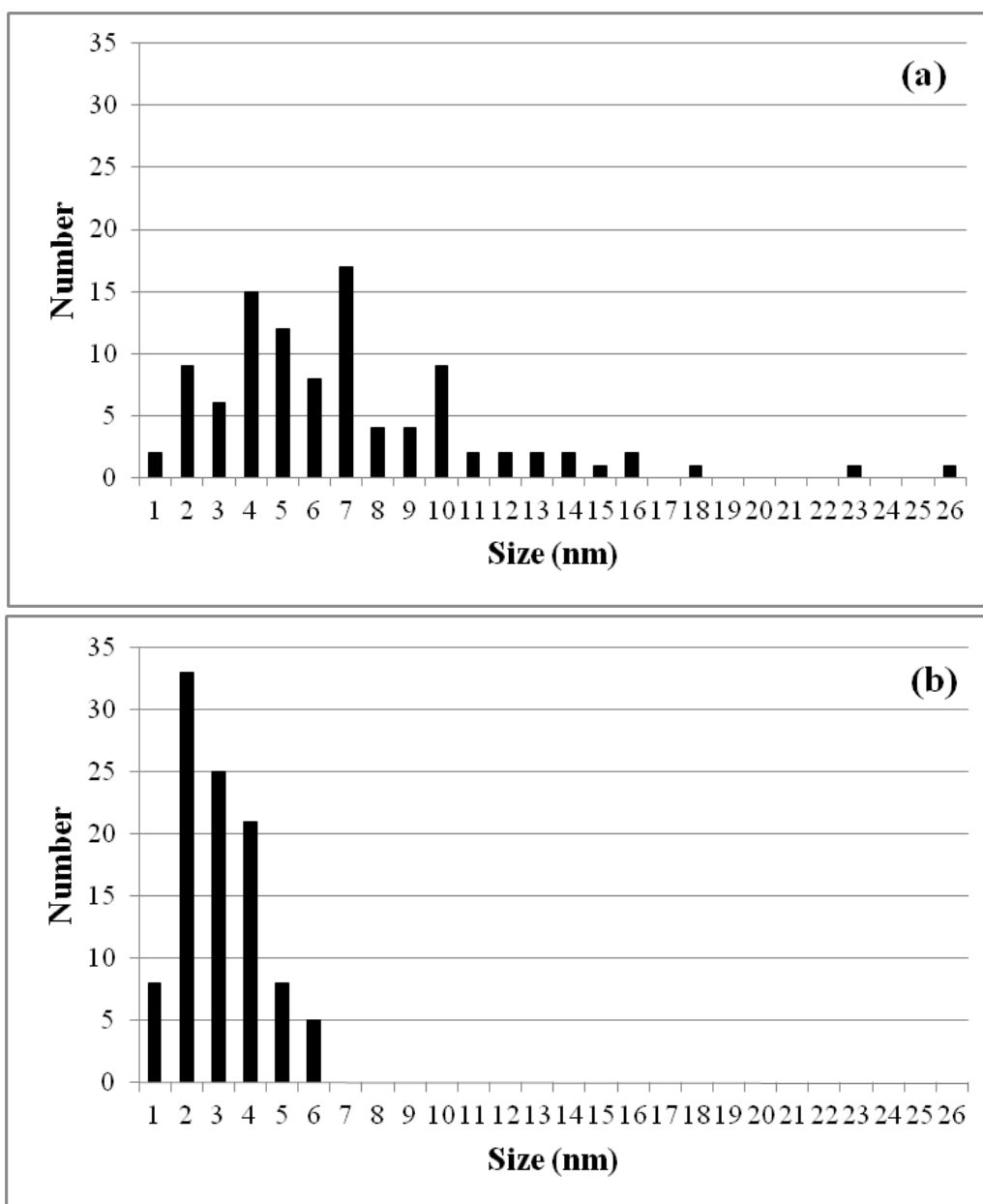


Fig. 4 Size distribution of nanoparticles prepared by laser wavelength of (a) 1064nm and (b) 532nm

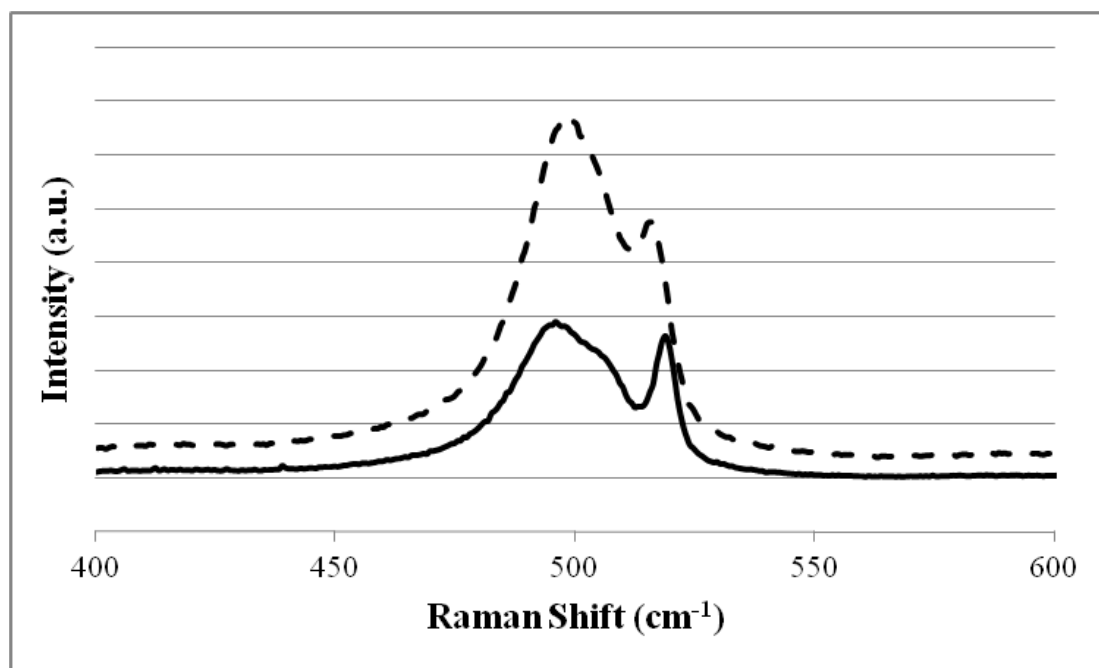


Fig. 5 Raman spectra of sample prepared by laser wavelength of 1064nm (solid line) and 532nm (dash line)

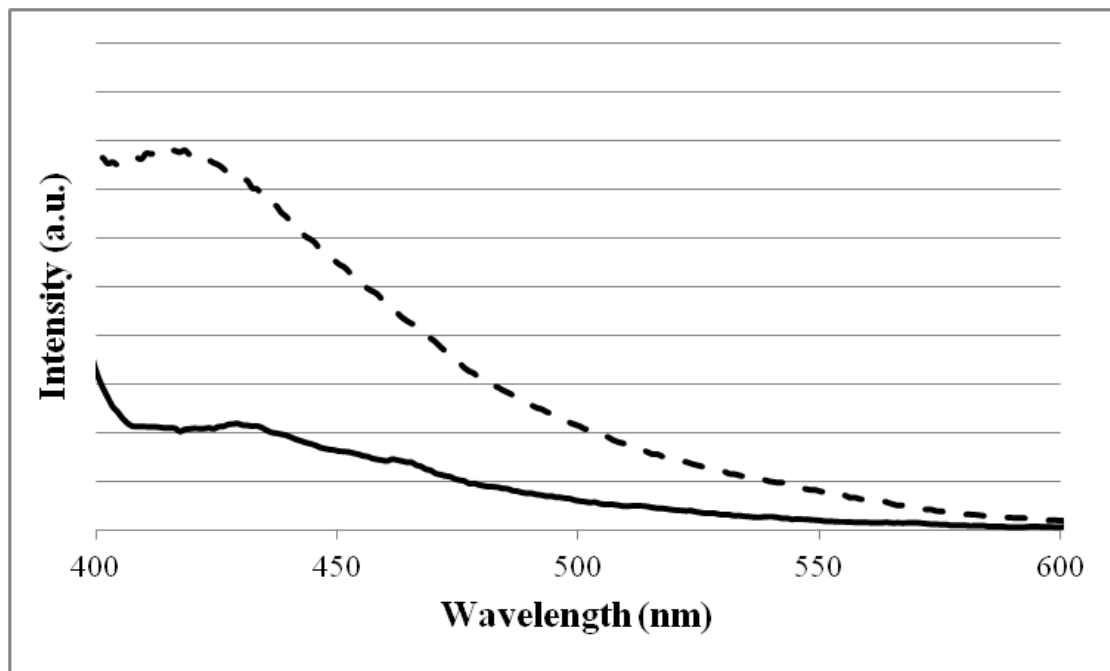


Fig. 6 PL spectra of sample prepared by laser wavelength of 1064nm (solid line) and 532nm (dash line)